AD-A138 276 MODELING CLIMATOLOGY OF AREAL COVERAGE(U) AIR FORCE 1/1
GEOPHYSICS LAB HANSCOM AFB MA I I GRINGORTEN 14 FEB 84
AFGL-TR-84-0053

UNCLASSIFIED F/G 4/2 NL

END
DATE FILMED
3 84
DTIC

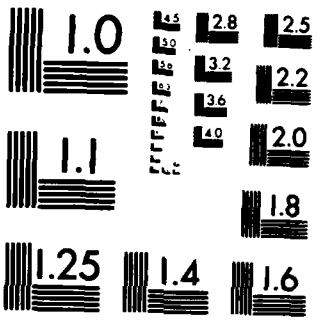

Unclassified
SECURITY CLASSIFICATION

AD A138276

(3)

REPORT DOCUMENTATION PAGE

1a. REPORT SECURITY CLASSIFICATION: Unclassified	1b. RESTRICTIVE MARKINGS
2a. SECURITY CLASSIFICATION AUTHORITY	3. DISTRIBUTION/AVAILABILITY OF REPORT: Approved for public release; distribution unlimited.
2b. DECLASSIFICATION/DOWNGRADING SCHEDULE	
4. PERFORMING ORGANIZATION REPORT NUMBER(S): AFGL-TR-84-0053	5. MONITORING ORGANIZATION REPORT NUMBER(S)
6a. NAME OF PERFORMING ORGANIZATION: Air Force Geophysics Lab; 6b. OFFICE SYMBOL (If applicable): LYT	7a. NAME OF MONITORING ORGANIZATION
6c. ADDRESS (City, State and ZIP Code): Hanscom AFB, Massachusetts 01731	7b. ADDRESS (City, State and ZIP Code)
8a. NAME OF FUNDING/SPONSORING ORGANIZATION; 8b. OFFICE SYMBOL (If applicable)	9. PROCUREMENT INSTRUMENT IDENTIFICATION NUMBER
8c. ADDRESS (City, State and ZIP Code)	10. SOURCE OF FUNDING NOS.

PROGRAM ELEMENT NO.	PROJECT NO.	TASK NO.	WORK UNIT NO.
62101F	6670	09	10

11. TITLE (Include Security Classification) (U)Modeling Climatology of Areal Coverage

12. PERSONAL AUTHOR(S): Irving I. Gringorten

13a. TYPE OF REPORT	13b. TIME COVERED	14. DATE OF REPORT (Yr., Mo., Day)	15. PAGE COUNT
REPRINT	FROM _____ TO _____	1984 February 14	8

16. SUPPLEMENTARY NOTATION: Presented at the Second International Meeting on Statistical Climatology, 26-30 Sep 1983, Lisbon, Portugal.

17. COSATI CODES		
FIELD	GROUP	SUB. GR.

18. SUBJECT TERMS (Continue on reverse if necessary and identify by block number): Cloud Cover; Climatic Probability; Areal Coverage; Simulation

19. ABSTRACT (Continue on reverse if necessary and identify by block number)

Several stochastic processes have been explored to simulate the areal climatic characteristics of the weather. The success or failure of a model of areal cover, or partial cover, has been judged partly by how well the resulting horizontal field of correlation resembles the natural field. The evaluation of each model, however, is based mostly on its efficiency in approximating the probability distribution of partial or complete coverage, by a weather condition, of an area. Emphasis, in application, is placed on the probability of cloud cover, that should vary from clear or zero cover, to partly cloudy, to overcast or 100% coverage. In addition to the size of the area, the probability distribution is directly related to the horizontal persistence of the weather element, which is parameterized in each model. The parameter is called scale distance. When the model successfully fits the observed areal extent, as viewed by a ground observer, it is then useful in application to other areal dimensions, as might be viewed by a satellite. With each of the several tested models, the "snapshot" picture of a field can be changed stochastically in

20. DISTRIBUTION/AVAILABILITY OF ABSTRACT	21. ABSTRACT SECURITY CLASSIFICATION
UNCLASSIFIED/UNLIMITED ☐ SAME AS RPT. ☐ OTIC USERS ☐	Unclassified

22a. NAME OF RESPONSIBLE INDIVIDUAL	22b. TELEPHONE NUMBER (Include Area Code)	22c. OFFICE SYMBOL
Irving I. Gringorten	(617) 861-5954	LY

DD FORM 1473, 83 APR — EDITION OF 1 JAN 73 IS OBSOLETE.

UNCLASSIFIED
SECURITY CLASSIFICATION OF THIS PAGE

DTIC FILE COPY

DTIC ELECTE FEB 23 1984 S D

84 02 21 105

a Markov process, simulating thereby a time sequence of weather patterns. Further investigation is well justified.

MODELING CLIMATOLOGY OF AREAL COVERAGE

Irving I. Gringorten

Air Force Geophysics Laboratory (LYT)
Hanscom AFB, MA 01731

1. INTRODUCTION

Throughout a given area, at any instant in time, the weather, such as rainfall depicted on a radar screen, or clouds in a satellite picture, produces a pattern that is unique to that instant in time, not likely to be duplicated at another instant. The change, from one instant to another, is likewise unique. Both the pattern and its change, however, are governed by basic restraints that characterize the climate of the area. The relevant climatology must consist of the statistics of the events or the probabilities of events in the area.

If the probability is known, say, of 24-hour rainfall exceeding 10 mm at a single observational point, we must ask: what is the corresponding probability that the same quantity will be exceeded everywhere in a surrounding area, or some fraction of a surrounding area? It is this type of climatology that is the subject of this paper.

Satellite pictures, recording as they do the areal coverage of cloudiness, eventually should help to provide the kind of cloud climatology that we seek. Radar has been a valuable asset in recent years because of the panoramic view that is provided of precipitation within a circular area surrounding the radar station. Satellite and radar, however, are recent tools. Generally, the existing climatic records contain single-instant observations of weather at single-point weather stations. Recorded rainfall amount is that at a rain gauge. Temperature is that in the thermometer shelter, and so on. The climatology of a city usually is that at an observational point in the city.

With respect to time, most observations might be considered as instantaneous, observed at regular intervals. But there are also time-integrated observations, like 24-hour totals of rainfall. There are observations of the average temperature, and maximum and minimum temperatures in a 24-hour period. All such observations contribute to the climatological character of a location as it relates to time or the duration of events. Is there a similar climatic record of spatial coverage of climate?

In most previous studies, correlation coefficients are the principal object of investigation, with notable exceptions. Schreiner and Riedel (1978) have collected rainfall data integrated over areas ranging in size from 26 km^2 to 2600 km^2, and have found frequencies of extremes of rainfall as a function of size of the ground covered. Other studies, by Court (1961), Briggs (1972) and Roberts (1971) have linked the rain in a circular area to the central single-station amounts by idealized models. In general, however, efforts at areal coverage have been few and models of areal coverage have been rare. The following examples illustrate the potential of such studies.

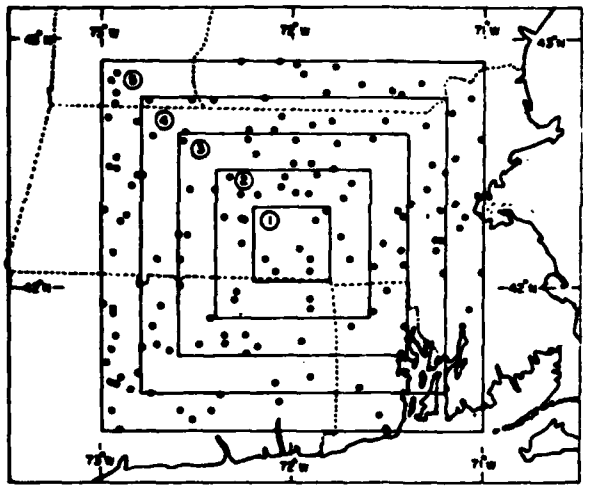

Fig. 1. A map showing the location of 145 stations equipped with rain gauges in New England.

Fig. 1 shows southern New England, centered in Massachusetts. There are 145 little circles showing locations of stations that report 24-hour rainfall. There are 5 nesting squares of areas ranging from 1000 km^2 to 28,000 km^2. Some 20 years of record have provided the estimates (Table 1) of the maximum 24-hour rainfall amounts as a function of areal size. The frequency of no rain at a single station is 62%, but within a sizeable area this frequency must drop steadily with increasing size of the area. The single-point probability of 25 mm of rain is 2.8%, or the probability that it will not be exceeded is 97.2%. As we look at areas of increasing size, this cumulative probability must decrease. Or conversely the prob-

Table 1. New England July maximum 24-hour rainfall, in square areas ranging in size from 1,000 km^2 to 28,000 km^2.

Rain Amount (mm)	Single-Station Frequ.	Frequency of Areal Maximum (Area in units of 10^3 km^2)		
		1	10	28
none	.62	.44	.17	.07
≤ 25	.97	.94	.76	.63
≤ 75	.999	.997	.984	.965

ability that rainfall will exceed 25 mm, somewhere in an area, must increase with increasing size of the area.

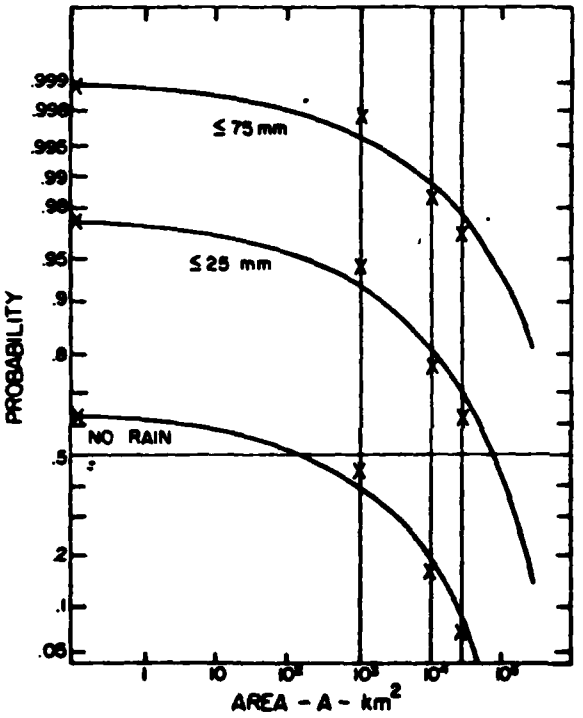

Fig. 2. The cumulative frequency of the maximum 24-hour rainfall in the areas of 10^3 km^2, 10^4 km^2 and 2.8×10^4 km^2, July in New England. The curves were fitted by a model of areal coverage.

The numbers that appear in Table 1 also appear in Fig. 2 at the X's. The solid curves have been drawn by means of a model of areal cover, which I shall try to describe shortly. In order to fit the curves to the observational data, a value had to be found for the model's parameter, called scale distance (2.63 km in the example). To understand this parameter, for the present, we describe it as the distance over which correlation coefficient is 0.99.

Another question is: What is the probability of rain over a fraction of the whole area? Fig. 3 is a sketch of one picture of a radar PPI-scope, showing scattered areas of stormy weather. Fig. 4 is a graphical presentation of frequencies of

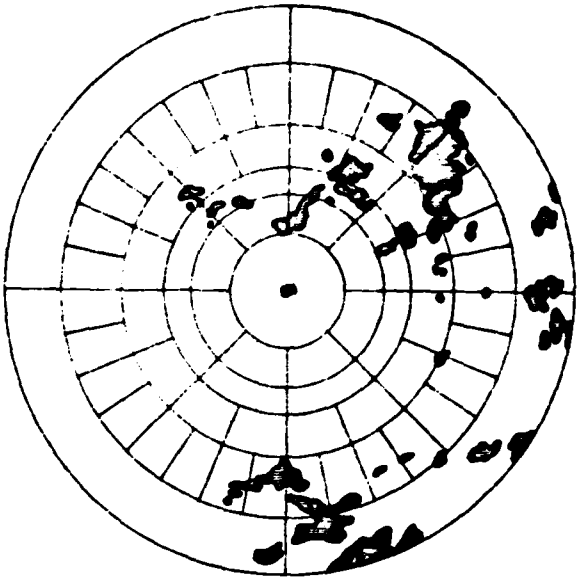

Fig. 3. Illustration of a PPI-radar picture, in which there were scattered storms producing radar echoes.

rainfall echoes. For example, at Key West, Florida, in summer, the single-point probability of a radar echo is 2%. But the radar sees rain over an area. We had divided the radar picture into cells, each cell of size 1580 km^2. Two cells have twice that area, all 64 cells have an area

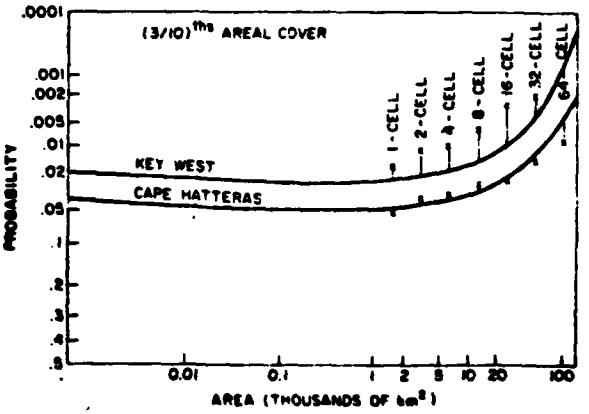

Fig. 4. The frequencies of radar echoes covering, at least, (3/10)ths of the areas ranging from 1.6×10^3 km^2 (1 cell) to 10^5 km^2 (64 cells). The plots are for Key West, Florida and Cape Hatteras, N.C. in summer (all hours included).

of approximately 100,000 km^2. The frequency of echoes, in at least 3/10ths of small areas, is nearly the same 2%. If the area becomes large, then a 2% singlepoint probability will not yield 30% cover very often. The solid curves of this diagram, again, are provided by a model of areal coverage.

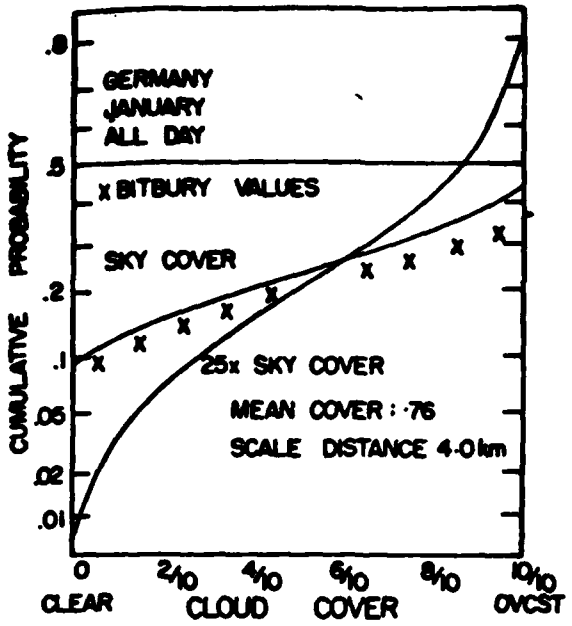

Fig. 5. The cumulative probability of cloud cover, from clear to overcast, for the area of the sky dome that an observer sees, and for 25 times that area. The example is for German stations with mean cloud cover 0.76 in January.

For partial cover let us look at Fig. 5, for an example of cloudiness. In this diagram we have plotted probabilities of cloud cover from clear to overcast. Germany has a satisfying high frequency of clouds in winter, averaging 76%. The summaries of ground observations at Bitburg are shown by the X's. The model provided a reasonable fit to this data, but the model does more. Consider a larger area that a satellite might see. Obviously the probability of all-clear must be less, likewise of complete overcast. The larger area must experience more cases of partial cover. The model provides such estimates that are otherwise not available.

One characteristic that we must simulate with our model is the change of correlation coefficient with the distance between stations. Fig. 6 is an example taken from a 1962 report (Bertoni and Lund). Correlation begins high for short distances, but drops to zero and becomes negative at substantial distances between stations. The example shows cc of surface temperatures plotted against distances between stations from a few km to several thousand km apart.

Theoretically an abundance of data, at an abundance of stations in a small area, with a rapid succession of observations, could provide the kind of areal climatology that we seek. Practically such abundance would confront us with the enormous task of mapping and recording events as a history of the weather, prior to its summarization

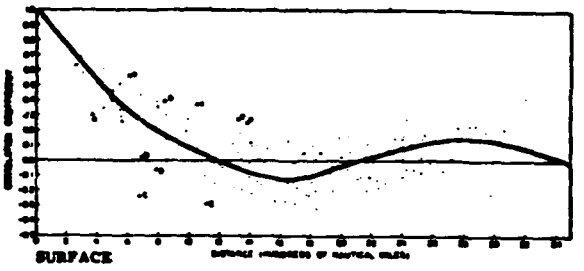

Fig. 6. Correlation coefficient versus distance between stations, of wintertime surface temperatures (Ref: Bertoni and Lund, 1964).

in statistical format. This is the difficulty that we wish to overcome by modeling. We want to be able to simulate a sequence of changes in the weather covering an area, whenever we choose, and we want, ultimately, to provide usable statistics of areal coverage, including cc's, and probabilities of fractional cover by weather conditions such as cloud cover.

By and large we must depend on statistical models which I must yet describe. But there is a concept that needs to be examined first, concerning the equivalent normal deviate.

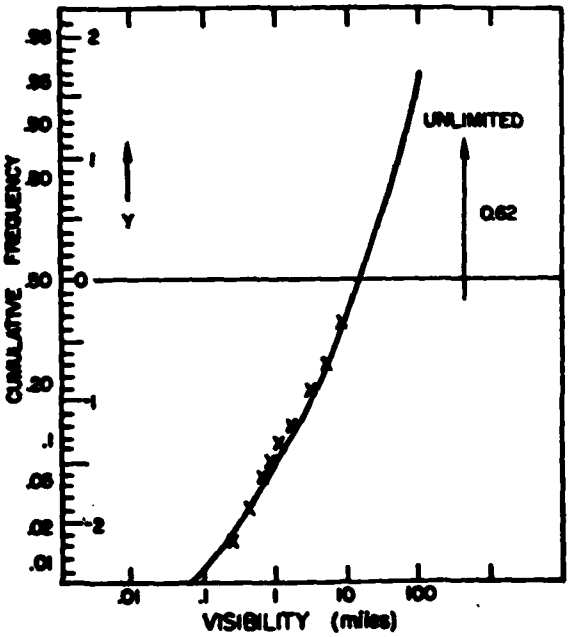

Fig. 7. Illustration of transformation of a weather element into its equivalent normal deviate (or vice versa). Example is for January noontime visibility at Bedford, MA.

2. EQUIVALENT NORMAL DEVIATE (END)

Fig. 7 is a sample plot of the cumulative frequency of a weather element, in this case of visibility at Bedford, MA, in January, at noontime. The X's mark the frequencies that have been summarized from 20 years of data. They show, for example, a frequency of 2% for visibility less than 1/4 mile, 7% for visibility less than 1 mile, also 62% frequency of visibility greater than 10 miles. Alongside the scale of cumulative probability we can plot another scale of the equivalent normal deviate, (y). The correspondence of y to F(y) can be found in nearly every textbook on statistics. By means of a diagram such as Fig. 7, or alternatively by equations, we obtain a transformation of the variable (V in this case) into its END (y), or vice versa.

Our models are derived using the END's. The results are then transformed to the appropriate weather variables, when so required.

3. APPROACH TO AREAL CLIMATOLOGY

An effective model of areal cover will produce a simulated horizontal field, stochastically, without recourse to physical laws or dynamics. Two early models (Gringorten, 1979) were devised in the manner illustrated in Fig. 8. Imagine that our horizontal space is filled with a fine-mesh grid of points. Assign, initially, random numbers to all points. Around point (i,j) draw a circle and take a weighted average of all the random numbers within the circle, then replace the random number at (i,j) with the weighted average, y(i,j). If we do this for all points within a large square, we shall obtain a pattern wherein the new values, at all points, will be correlated with each other. Models that have been composed in this way differ from each other in the weighting function that is selected for each model.

Once a model is selected, the adopted procedure can be repeated many times to produce many simulated synoptic situations, thus comprising a large sample that can be surveyed for spatial correlations or associations.

This early modeling procedure has been set aside in favor of a new model that requires the generation of only a few dozen random numbers per map, instead of many thousands.

4. BOEHI'S SAWTOOTH WAVE MODEL (BSW)

The presently preferred model was devised by Major Albert R. Boehm, USAF. He has given it the descriptive name Sawtooth Wave. We shall refer to it as the BSW-model.

We begin with a horizontal space (Fig. 9) with axes (U,V) and point of origin (0,0). We introduce a stationary wave formation with waves that are straight and uniform in wavelength. The wavelength (A) becomes the parameter of the model, which, in our climatic fields, measures several hundred to several thousand km. In the following derivation, however, the wavelength is the unit of distance.

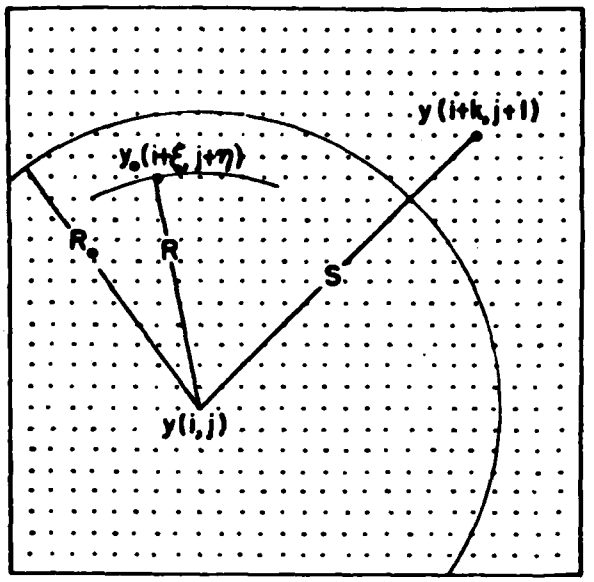

Fig. 8. To illustrate the former development of stochastic modeling.

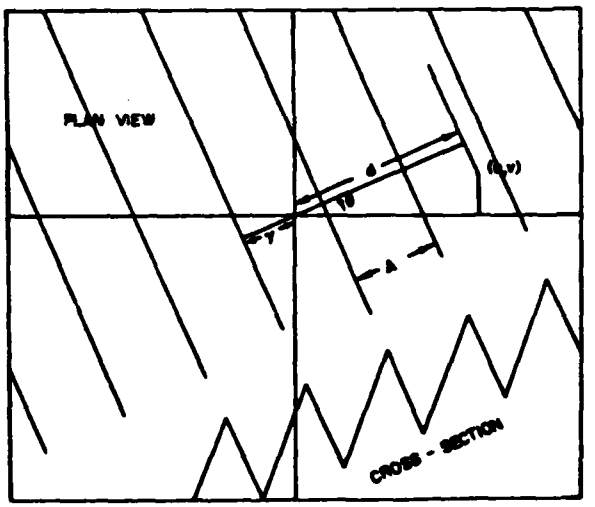

Fig. 9. To illustrate the stochastic procedure in the BSW-model.

In cross-section the waves are saw-tooth in form. The left-hand edge of each wave has zero height, the right-hand edge has a height of unity. At any point (u,v) in between the wave phase, $\pi(u,v)$, is uniformly distributed between zero and one.

The wave formation has two degrees of freedom, and thus allows for selection of two random numbers: one for the direction (θ) of the wave formation and one for the phase at the point of origin, $\pi(0,0)$, which must be equal to the fractional distance γ shown in the diagram. At every point in the U-V field there is a wave phase, $\pi(u,v)$.

Now, consider many (N) wave formations, each with a random direction (θ_i) and each with a random phase (γ_i) at the origin. Then, at each point (u,v) there will be N values of

$$x_i(u,v) \text{ for } 1 \leq i \leq N$$
$$0 \leq \theta_i \leq 2\pi$$
$$0 \leq \gamma_i \leq 1$$

The average, y(u,v), of all N values of $x_i(u,v)$, as N becomes large, will have an asymptotically Gaussian distribution. When, for convenience, N is made equal to 12, the equation becomes

$$y(u,v) = \sum_{i=1}^{12} x_i(u,v) - 6$$

There will be a value of y(u,v) at each point (u,v) in the horizontal space. A sample of such generated fields is shown in Fig. 10, with distinct low and high cells and saddle points.

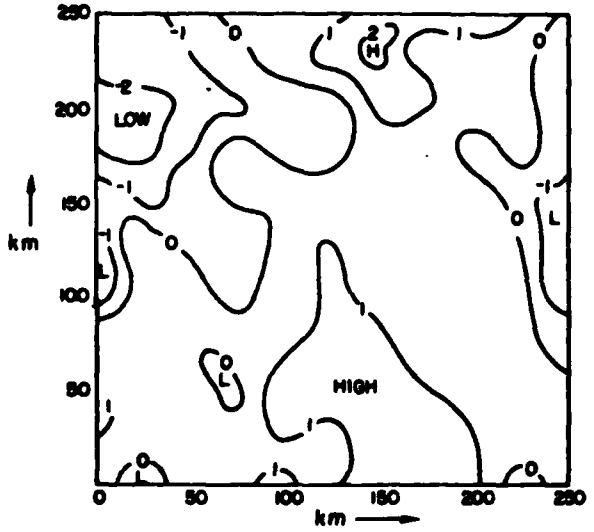

Fig. 10. Example of horizontal field generated stochastically by the BSW-model.

4a. Correlation

An analytical solution has been found for the correlation coefficient $\rho(s)$ between points separated by distance (s), in units of the wavelength:

$$\rho(s) = 3s^2 - (12/\pi)s + 1 \qquad \text{for } 0 \leq s \leq 1$$
$$= 3s^2 - (12/\pi)s + 1 + (24/\pi)[\cos^{-1}(1/s) - \sqrt{s^2-1}] \qquad \text{for } 1 \leq s \leq 2$$

The graph of $\rho(s)$ versus s is shown in Fig. 11. For our purposes we shall rarely need to consider distances of more than one wavelength. The distance (s) will usually be a number between zero and one, given by

$$s = s'/A$$

where s' is the distance (km) and A is the parameter wavelength (km).

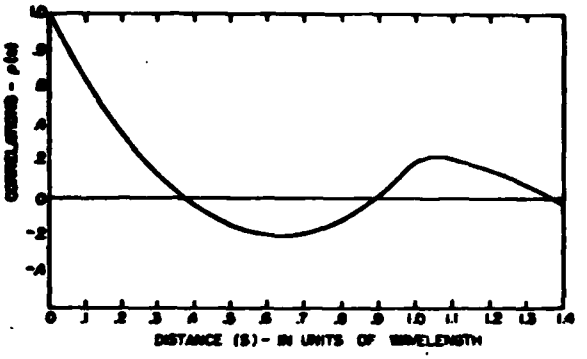

Fig. 11. Graphical presentation of the change of cc with distance in the BSW model.

4b. Areal coverage

While we have an analytical solution for the correlation decrease with distance we lack such good fortune, at this time, for the primary goal of this paper: to find the probability of the maximum condition in an area or a fraction of the area. We have obtained approximate, although good, solutions by Monte Carlo simulation. The following is a brief description of our procedures.

In a field generated by the model, consider a square area of side s (in units of the wavelength). At some point in the area (s^2) there will be a maximum. There will be, also, a tenth largest, a two-tenths largest, --- and finally the minimum in the area. In terms of a fraction (f) of the area the maximized minimum in such fraction, $y(f,s^2)$, becomes the primary subject. We want to find the cumulative probability distribution of the threshold value: $P(y:f,s^2)$.

A large number (M) of stochastically generated maps will provide a frequency distribution of $y(f,s^2)$ that will approach the true probability distribution asymptotically as M is increased.

This kind of Monte Carlo simulation was conducted with M = 25,000. On each map 12 square areas were surveyed for the largest value of y, the (1/10)th largest, (2/10)th largest, and so on, down to the smallest value. The linear size of each square, in units of wavelength, was

$$s = 2^z/340 \qquad \text{where } z = -1(1)10$$

From all 25,000 maps cumulative frequencies were found for each

$$y(f,s^2) = -3.5(0.5)3.5$$

for $f = 0(0.1)1.0$

and $z = -1(1)10$.

Using the frequencies thus obtained the charts of Fig. 12 were drawn to show the probability estimates of y-maxima for f = 0.0, 0.1, 0.3, 0.5 successively, and for s from -1 to 8. Smoothing was necessary, especially at the extremes of the distributions.

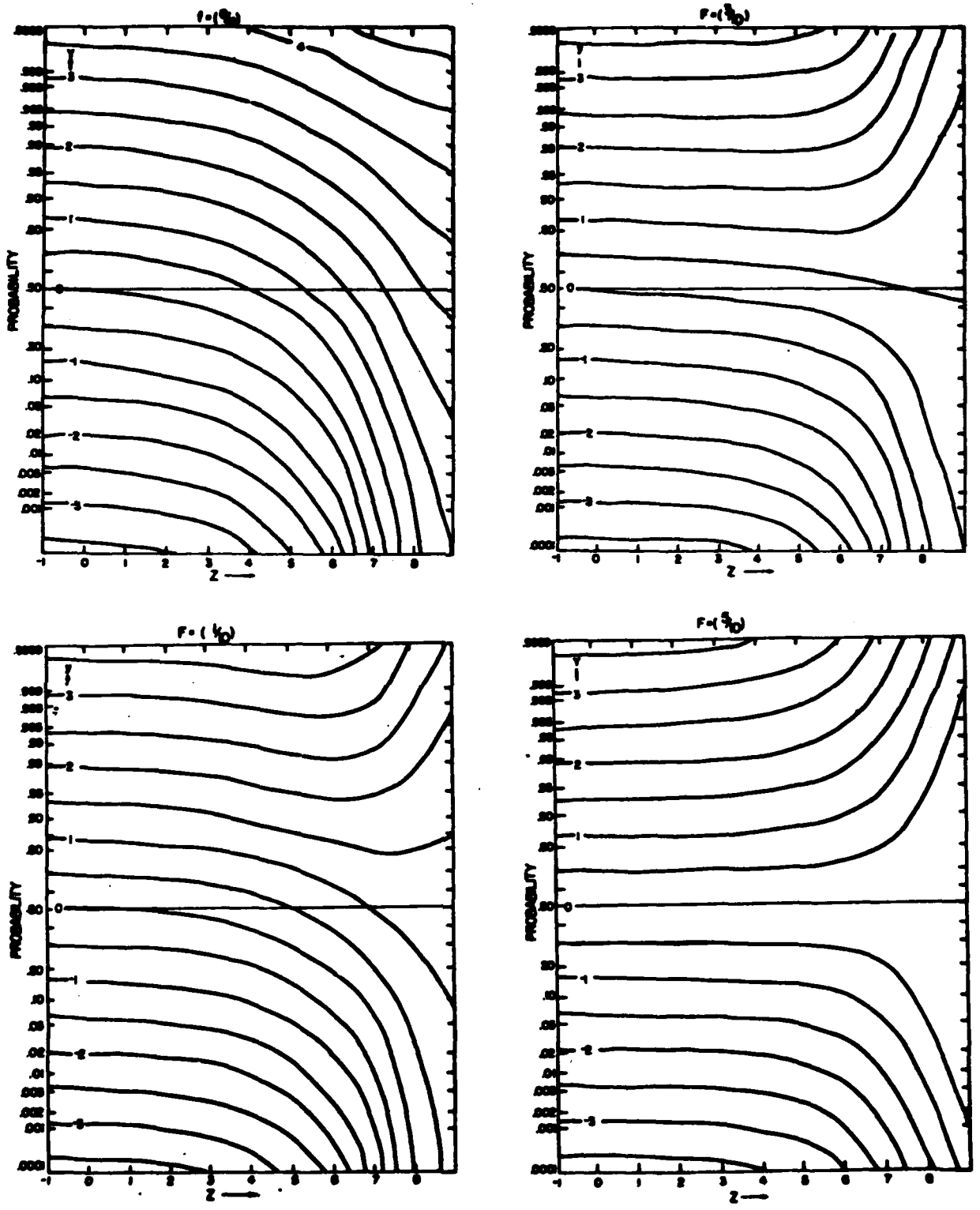

Fig. 12. SSW-model charts of the probabilities, $P(y;f,a^2)$, of fractional cover (f) of an area (a^2) of EHD-values not exceeding y.

4c. Applications

For a square area, A km^2, with linear dimension s' km we set

$$s = s'/A$$

for which

$$z = \ln(340s)/\ln 2$$

When z is entered in a chart of Fig. 12, the vertical line upward from the abscissa provides estimates of the probabilities of various thresholds of y corresponding to the area (A).

Instead of the wavelength (A) it is convenient to substitute the parameter (r), called the scale distance. In the BSW-model it is a distance over which the cc is 0.9888 (close to 0.99). By and large, it is a more meaningful parameter in application, given by

$$r = s'/340s \text{ km} = A/340 \text{ km} = \sqrt{A}/2^z \text{ km}.$$

Or, for z:

$$z = \ln(\sqrt{A}/r)/\ln 2$$

For the New England 24-hour winter precipitation, we found scale distances of 9 to 10 km. For radar echoes they ranged from 1 to 2 km in summer, 2 1/2 to 4 1/2 km in winter. Cloud cover scale distances have ranged from 1/2 km to 10 km depending on season, time of day as well as geographic location. [2]

5. TIME CHANGES

The above-described model enables us to generate "snapshot" pictures stochastically of a horizontal field. So, far, the END-value y(u,v) at a point (u,v) on one map is independent of that generated on any other map.

Let us suppose that one map has been generated at time t with values of $y_t(u,v)$ at each point (u,v) of the space. Let another map be generated, for the time (t+δt), in terms of an END (η) to give values of $\eta_{(t+\delta t)}(u,v)$ at each point (u,v). Make the modification to $y_{(t+\delta t)}(u,v)$ by means of the Markov model:

$$y_{(t+\delta t)}(u,v) = \rho_t \cdot y_t(u,v) + \sqrt{1-\rho_t^2} \cdot \eta_{(t+\delta t)}(u,v)$$

where the cc (ρ_t) for time lag (δt) is given by

$$\rho_t = \exp(-t/T)$$

where T (in hours) is a parameter called relaxation time.

Between the y-values of the later map, the cc can be proved to be still ρ(s), the same as it was on the map at time t. That is, the cc-field on the new map, δt hours later, is preserved. This is a necessary condition to assure the continuity of the model's characteristics. An example of hourly changes is shown in Figs. 13 for T = 20 hours.

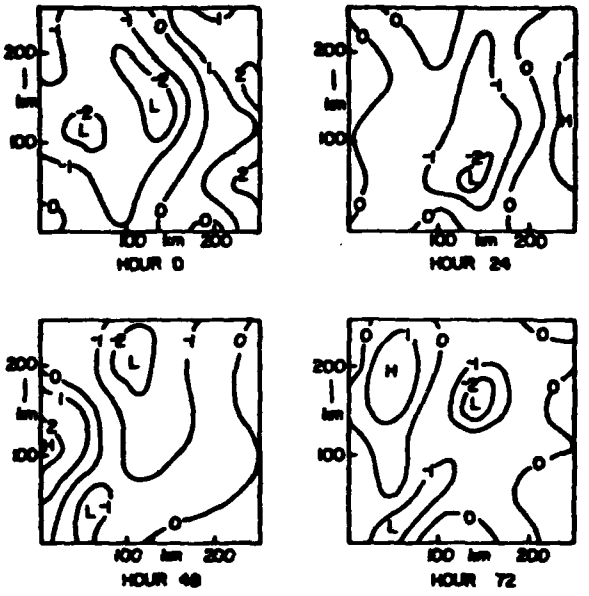

Fig. 13. Example of stochastic horizontal fields following one another at 24-hour intervals in a Markov process.

6. *REMAINING PROBLEMS*

These efforts have raised more problems than they have solved. We have devised a procedure to generate synoptic pictures of the weather, stochastically, without regard for the underlying physical processes. We have made no effort to use the models of Numerical Weather Prediction (NWP) to produce successive pictures of the meteorological events. At this time, however, we do not know if the hourly sequences of NWP will, in fact, yield a climatology that approximates that of the real climate with respect to such elements as cloud cover, especially mesoscale features. At this point in time we are justified in adopting a procedure that will produce maps that, collectively, will yield a climatology consisting of a good approximation to the horizontal field of correlation and satisfactory probability estimates of the maximum and minimum of the weather conditions in fraction (f) of an area (A). There is nothing in the model, yet, that will cause a synoptic situation to be advected as well as modified. An ultimate model should be 4-dimensional, to yield probabilities of conditions in 3-dimensional space and to include events in time. Moreover, the probability of events or conditions should be estimated analytically instead of by Monte Carlo simulation. We have made a beginning, but much remains to be done.

7. ACKNOWLEDGEMENTS

The author's associates, Donald D. Grantham and Charles Burger, have contributed generously to the substance of this paper and have provided critical insight into the problems. The Sawtooth Wave Model is the invention of Major Albert R. Boehm, USAF, Environmental Technical Applications Center. Much of the background effort was performed by the computer division, AFGL, and by students of Regis College, Weston, MA.

8. REFERENCES

Bertoni, E. A., and Lund, E. A., 1964: Winter space correlations of pressure, temperature and density to 16 km. Environ. Res. Pap., No. 75, AFCRL-64-1020.

Brigge, J., 1972: Probability of aircraft encounters with heavy rain. Meterol. Mag., 101, pp 8-13.

Court, A., 1961: Area-depth rainfall formulas. J. Geophys. Res., 66, pp 1823-1831.

Gringorten, I. I., 1979: Probability models of weather conditions occupying a line or an area. J. of Appl. Meteorol., 18, pp 957-977.

National Bureau of Standards, 1961: Handbook of Mathematical Functions, Applied Mathematics Series, 55, Government Printing Office, Washington, D.C., 1045 pp.

Roberts, C. F., 1971: A note of the derivation of a scale measure for precipitation events. Mon. Wea. Rev., 99, pp 873-876.

Schreiner, L. C. and Riedel, J. F., 1978: Probable maximum precipitation estimates United States east of 105th meridian, Hydrometeo. Rep. No. 51, NOAA-NWS-HR-51.